

Pion Electroproduction from Nuclei*

E. J. MONIZ†

Institute of Theoretical Physics, Department of Physics, Stanford University, Stanford, California 94305

(Received 18 February 1969)

Detailed understanding of hadron production in nuclei is important for nuclear physics, for the study of hadron-nucleon interactions, and for quantum-electrodynamic experiments involving nuclear targets. The double differential electron-nuclear cross section is calculated for the region of electron energy loss corresponding to excitation of the first nucleon resonance, using a Fermi-gas model of the nucleus. This simple model allows us to reach an analytic expression for the cross section and to tie directly onto the Czyz-Walecka threshold calculation. Further, the quasielastic scattering is calculated in exactly the same nuclear model to indicate the reliability of this approach. Since the results here are model-dependent, such experiments should allow some insight into the nuclear physics.

I. INTRODUCTION

THERE is strong motivation to investigate the production of hadrons in nuclei: One would like to understand the nuclear physics of the production process and eventually to use nuclei as targets for studying hadron-nucleon interactions. This is perhaps the only presently feasible way to examine in detail the interactions of very short-lived particles and resonances. Here we consider inelastic scattering of electrons from nuclei in the region of excitation energy corresponding to the first nucleon resonance and make a first attempt to compute the cross section in this region. The advantages in using electrons are that the basic interaction between the electron and the target nucleus is known and that we have both the three-momentum transfer to the nucleus \mathbf{q} and the energy loss ω of the electron as variables, the only requirement being that $q^2 = q_\mu^2 = \mathbf{q}^2 - \omega^2$ be spacelike.

Furthermore, if one detects only the final electron, then any electrodynamic process connected by one-photon exchange with the nucleus can be described by only two form factors, $W_{1,2}(q^2, q \cdot P)$.^{1,2} Knowledge of these functions is essential to anyone carrying out quantum-electrodynamic experiments with nuclear targets; electron scattering allows us to map out the form factors in the relevant region: $q^2 > 0$, $q \cdot p < -\frac{1}{2}q^2$. The quasielastic scattering contribution to these form factors has been calculated by several authors,²⁻⁴ while Czyz and Walecka⁵ have estimated the contribution from single-pion electroproduction in the region of electron energy loss just above meson threshold. We now extend these estimates up through the N^* (1236).

It should also be noted that separation of the strictly nuclear effects from meson production is itself import-

ant, since information on short-range nucleon-nucleon correlations is contained in the high energy-loss tail of the quasielastic peak.⁶ In addition, the usual sum rules for electron scattering^{7,8} do not include mesonic degrees of freedom.

In anticipation of experiments to be carried out into the region of pion production, we look at electron scattering from a free Fermi gas in the Born approximation. This rather simple model allows us to reach an analytic expression that should at least reproduce the gross features of the inelastic cross section and also to tie directly onto the threshold results of Czyz and Walecka (who use the same Fermi-gas nuclear excitation spectrum). To give us some indication of the reliability of this approach, the quasielastic scattering is calculated in exactly the same nuclear model: The electron is considered to scatter elastically from a single nucleon in the Fermi sea, the recoiling nucleon lying outside the Fermi sphere because of the exclusion principle. Most importantly, for mesons near the 3-3 resonance, the strong final-state interaction is simulated by a nucleon isobar, treated as a discrete state. That is, electromagnetic excitation of the P_{33} resonance is assumed to dominate single-pion production in this region. Therefore, the calculation differs from the quasielastic only in that the elastic nucleon-nucleon vertex is replaced by the nucleon-isobar electromagnetic vertex.

II. ELECTRON-NUCLEUS CROSS SECTION

We now proceed to analyze the general electron-nucleus scattering process in the one-photon exchange approximation (Fig. 1), with only the final electron detected. The usual Feynman rules yield the cross section

$$d^2\sigma = 2Z^2\alpha^2 (d\mathbf{p}_2/2\epsilon_2) q^{-4} W_{\mu\nu} N_{\mu\nu} [(p_1 \cdot P)^2 - m^2 M_T^2]^{-1}, \quad (1)$$

where m is the electron mass, M_T is the target (nuclear)

* Research sponsored by the Air Force Office of Scientific Research, Office of Aerospace Research, U.S. Air Force, under AFOSR Contract No. F44620-68-C-0075.

† National Science Foundation Predoctoral Fellow.

¹ S. D. Drell and J. D. Walecka, *Ann. Phys. (N.Y.)* **28**, 18 (1964).

² T. deForest and J. D. Walecka, *Advan. Phys.* **15**, 1 (1966).

³ W. Czyz, *Phys. Rev.* **131**, 2141 (1963).

⁴ G. R. Henry, *Phys. Rev.* **151**, 875 (1966).

⁵ W. Czyz and J. D. Walecka, *Nucl. Phys.* **51**, 312 (1964).

⁶ W. Czyz and K. Gottfried, *Ann. Phys. (N.Y.)* **21**, 47 (1963).

⁷ S. D. Drell and C. L. Schwartz, *Phys. Rev.* **112**, 568 (1958).

⁸ K. W. McVoy and L. Van Hove, *Phys. Rev.* **125**, 1034 (1962).

mass, and

$$N_{\mu\nu} \equiv -\frac{1}{2} \text{Tr}[\gamma_\mu(m - i\mathbf{p}_1)\gamma_\nu(m - i\mathbf{p}_2)],$$

$$W_{\mu\nu} \equiv [(2\pi)^3\Omega/Z^2] \sum'_{\text{initial state}} \sum_{\text{final state}} \delta^{(4)}(P' - P - q)$$

$$\times \langle P | J_\nu(0) | P' \rangle \langle P' | J_\mu(0) | P \rangle (E), \quad (2)$$

where Ω is the normalization volume, E is the initial target energy, $|P\rangle$ and $|P'\rangle$ are the Heisenberg state vectors of the initial and final nuclear states, respectively, $J_\mu(0)$ is the electromagnetic-current operator of the strongly interacting system at $x_\mu=0$ and \sum' indicates an average over the initial target states. Now, covariance, parity conservation, and current conservation imply⁹⁻¹¹

$$W_{\mu\nu} = W_1(q^2, q \cdot P) \left(\delta_{\mu\nu} - \frac{q_\mu q_\nu}{q^2} \right) + W_2(q^2, q \cdot P)$$

$$\times \frac{1}{M_T^2} \left(P_\mu - \frac{q \cdot P}{q^2} q_\mu \right) \left(P_\nu - \frac{q \cdot P}{q^2} q_\nu \right). \quad (3)$$

But q_μ gives zero when contracted with the electron current, and $q^2 = \mathbf{q}^2 - \omega^2$ and $q \cdot P = -\omega M_T$ for the three-momentum transfer to the nucleus \mathbf{q} and the electron energy loss in the laboratory system ω . Therefore,

$$W_{\mu\nu} = W_1(q^2, \omega) \delta_{\mu\nu} - W_2(q^2, \omega) \delta_{\mu 4} \delta_{\nu 4} \quad (4)$$

in the lab system, giving the lab cross section

$$d^2\sigma/d\Omega_2 d\epsilon_2 = (Z^2 \sigma_M / M_T)$$

$$\times [W_2(q^2, \omega) + 2W_1(q^2, \omega) \tan^2 \frac{1}{2}\theta], \quad (5)$$

where $\sigma_M = (\alpha^2 \cos^2 \frac{1}{2}\theta) / 4\epsilon_1^2 \sin^4 \frac{1}{2}\theta$ is the Mott cross section, and we have neglected the mass of the electron. We must now evaluate the form factors $W_{1,2}$ for quasi-elastic scattering and for meson production.

A. Quasielastic Scattering

Our model for quasielastic scattering is simply that the electron scatters from a single nucleon in the free Fermi sea, with the recoiling nucleon required to lie outside the Fermi sphere. In other words, because of the Pauli principle, the nucleon cannot scatter into an already occupied state. In short, our model for the nuclear transition current is, in the lab frame,

$$J_\mu = \sum_{\mathbf{k}\lambda} a_{\mathbf{k}+\mathbf{q}\lambda'}^\dagger \langle \mathbf{k}+\mathbf{q}\lambda' | j_\mu | \mathbf{k}\lambda \rangle$$

$$\times a_{\mathbf{k}\lambda} \theta(k_F - |\mathbf{k}|) \theta(|\mathbf{k}+\mathbf{q}| - k_F), \quad (6)$$

where $a_{\mathbf{k}\lambda}$ ($a_{\mathbf{k}\lambda}^\dagger$) is a free-nucleon annihilation (creation) operator, and the matrix element is that for the free-nucleon electromagnetic vertex:

$$(\Omega^2 EE')^{1/2} \langle k' = k + q | j_\mu(0) | k \rangle = iM u(k')$$

$$\times [F_1(q^2) \gamma_\mu - F_2(q^2) \sigma_{\mu\nu} q_\nu] u(k).$$

We are now in a position to evaluate the tensor $W_{\mu\nu}$. Inserting the above expressions into Eq. (2), and con-

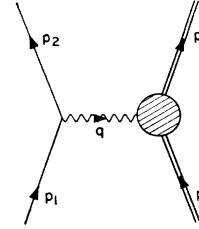


FIG. 1. Electron scattering process in lowest order in α .

sidering only the case $Z = N = \frac{1}{2}A$,¹²

$$W_{\mu\nu} = \frac{3M_T}{4\pi A k_F^3}$$

$$\times \int d\mathbf{k} \delta(\omega + \epsilon_{\mathbf{k}} - \epsilon_{\mathbf{k}+\mathbf{q}}) \theta(k_F - |\mathbf{k}|) \theta(|\mathbf{k}+\mathbf{q}| - k_F)$$

$$\times \sum_{\lambda\lambda'} \Omega^2 [\langle \mathbf{k}+\mathbf{q}\lambda' | j_\mu^n(0) | \mathbf{k}\lambda \rangle \langle \mathbf{k}\lambda | j_\nu^n(0) | \mathbf{k}+\mathbf{q}\lambda' \rangle$$

$$+ \langle \mathbf{k}+\mathbf{q}\lambda' | j_\mu^p(0) | \mathbf{k}\lambda \rangle \langle \mathbf{k}\lambda | j_\nu^p(0) | \mathbf{k}+\mathbf{q}\lambda' \rangle], \quad (7)$$

where the superscripts n and p indicate neutron and proton, respectively. Upon performing the traces, we have

$$W_{\mu\nu} = \frac{3M_T}{4\pi A k_F^3}$$

$$\times \int d\mathbf{k} \frac{\delta(\omega + \epsilon_{\mathbf{k}} - \epsilon_{\mathbf{k}+\mathbf{q}}) \theta(k_F - |\mathbf{k}|) \theta(|\mathbf{k}+\mathbf{q}| - k_F)}{\epsilon_{\mathbf{k}} \epsilon_{\mathbf{k}+\mathbf{q}}}$$

$$\times \left[T_1(q^2) \left(\delta_{\mu\nu} - \frac{q_\mu q_\nu}{q^2} \right) \right.$$

$$\left. + T_2(q^2) \frac{1}{M^2} \left(k_\mu - \frac{q \cdot k}{q^2} q_\mu \right) \left(k_\nu - \frac{q \cdot k}{q^2} q_\nu \right) \right], \quad (8)$$

with

$$T_1(q^2) = \frac{1}{2} q^2 (F_1^p + 2MF_2^p)^2 + \frac{1}{2} q^2 (F_1^n + 2MF_2^n)^2,$$

$$T_2(q^2) = 2M^2 (F_1^p)^2 + q^2 (F_2^p)^2 + 2M^2 (F_1^n)^2 + q^2 (F_2^n)^2. \quad (9)$$

The similarity between Eq. (3) and the quantity in square brackets in Eq. (8) should be noted. This form is to be expected by the same argument of covariance and current conservation which led to Eq. (3), except that the form factors $T_{1,2}$ depend only on q^2 . (This is because $q \cdot k$ and q^2 are not independent when a discrete final state is considered.) This observation will be important in considering isobar production, where the traces are much more tedious.

Once again we drop the terms in q_μ through contraction with the electron current. Next we identify the remaining terms in Eq. (8), which is valid in the lab frame, with those of Eq. (4), the reduction of $W_{\mu\nu}$ in the lab frame, and thereby separate out W_1 and W_2 . Choosing the three-momentum transfer \mathbf{q} as the polar

⁹ R. Von Gehlen, Phys. Rev. **118**, 1455 (1960).

¹⁰ M. Gourdin, Nuovo Cimento **21**, 1004 (1961).

¹¹ J. D. Bjorken, 1960 (unpublished).

¹² All results will be presented for $Z = N = \frac{1}{2}A$. The general case is easily recovered.

axis, and denoting the polar angle by τ , we have

$$W_1(\mathbf{q}^2, \omega) = \frac{3M_T}{4\pi A k_F^3} \times \int d\mathbf{k} \frac{\delta(\omega + \epsilon_{\mathbf{k}} - \epsilon_{\mathbf{k}+\mathbf{q}}) \theta(k_F - |\mathbf{k}|) \theta(|\mathbf{k}+\mathbf{q}| - k_F)}{\epsilon_{\mathbf{k}} \epsilon_{\mathbf{k}+\mathbf{q}}} \times [T_1(q^2) + (1/2M^2) T_2(q^2) k^2 \sin^2 \tau],$$

$$W_2(\mathbf{q}^2, \omega) = \frac{3M_T}{4\pi A k_F^3} \frac{T_2(q^2)}{M^2} \times \int d\mathbf{k} \frac{\delta(\omega + \epsilon_{\mathbf{k}} - \epsilon_{\mathbf{k}+\mathbf{q}}) \theta(k_F - |\mathbf{k}|) \theta(|\mathbf{k}+\mathbf{q}| - k_F)}{\epsilon_{\mathbf{k}} \epsilon_{\mathbf{k}+\mathbf{q}}} \times \left[\left(\epsilon_{\mathbf{k}} - \frac{\omega}{|\mathbf{q}|} k \cos \tau \right)^2 + \frac{1}{2} \frac{q^2}{|\mathbf{q}|^2} k^2 \sin^2 \tau \right]. \quad (10)$$

We first employ nonrelativistic kinematics both for the target nucleons ($k_F \approx \frac{1}{4}M$) and for the recoil nucleons (this will be good for small $|\mathbf{q}|$), retaining only leading order terms in $|\mathbf{k}|/M$ in the integrand. We take account of the k^2 dependence of the binding of the target nucleons by allowing for an effective mass M^* . For small energy loss, we also use the same effective mass for the recoiling nucleons; i.e., they still experience the nuclear matter potential. This does not give a proper treatment of the threshold region but rather an average description in the region of discrete levels. The energy-conserving δ function then becomes $\delta(\omega - |\mathbf{q}|^2/2M^* - \mathbf{k} \cdot \mathbf{q}/M^*)$, which, because of the finite momentum distribution, causes the cross section to vanish identically outside $\omega_{\min} < \omega < \omega_{\max}$, where

$$\omega_{\max} = [|\mathbf{q}|^2/2M^* + |\mathbf{q}| k_F/M^*],$$

$$\omega_{\min} = \theta(|\mathbf{q}| - 2k_F) [|\mathbf{q}|^2/2M^* - |\mathbf{q}| k_F/M^*].$$

Clearly, a tail in the momentum distribution introduces a tail into the quasielastic cross section. Performing the angular integrations we have

$$W_1(\mathbf{q}^2, \omega) = \frac{3M_T}{4\pi A} \left(\frac{2\Omega}{3\pi^2 A} \right) \frac{M^*}{M(M+\omega)} \frac{2\pi}{|\mathbf{q}|} \times \int_0^\infty dk kn(k) [1 - n((k^2 + 2M^*\omega)^{1/2})] \times \left\{ T_1(q^2) + \frac{1}{2} \frac{T_2(q^2)}{M^2} \left[k^2 - \left(\frac{M^*\omega}{|\mathbf{q}|} - \frac{|\mathbf{q}|}{2} \right)^2 \right] \right\},$$

$$W_2(\mathbf{q}^2, \omega) = \frac{3M_T}{4\pi A} \left(\frac{2\Omega}{3\pi^2 A} \right) \frac{T_2(q^2)}{M^2} \frac{M^*}{M(M+\omega)} \frac{2\pi}{|\mathbf{q}|} \times \int_0^\infty dk kn(k) [1 - n((k^2 + 2M^*\omega)^{1/2})] \times \left\{ \left[M - \frac{\omega}{|\mathbf{q}|} \left(\frac{M^*\omega}{|\mathbf{q}|} - \frac{|\mathbf{q}|}{2} \right) \right]^2 + \frac{1}{2} \frac{q^2}{|\mathbf{q}|^2} \times \left[k^2 - \left(\frac{M^*\omega}{|\mathbf{q}|} - \frac{|\mathbf{q}|}{2} \right)^2 \right] \right\}. \quad (11)$$

Here $n(k) = \theta(k_F - k)$ for the Fermi distribution; i.e., $n(k)$ is the occupation-number distribution of plane-wave states. The normalization volume Ω is defined by relation

$$4 \frac{\Omega}{(2\pi)^3} \int d\mathbf{k} n(k) = A.$$

At this point we could insert some distribution (spherical in momentum space) other than a Fermi gas and perform the integrals numerically. For a shell-model nucleus, we have $n(k) = \sum_{nlm} n_{nlm}(k)$, where the sum is over the occupied levels; for a harmonic-oscillator potential, we have for the $n=1$ and $n=2$ shells

$$n_{1lm}(k) = \delta_{m,0} \frac{2^l}{(2l-1)!!} \left(\frac{k}{k_0} \right)^{2l} \exp\left(-\frac{k^2}{k_0^2}\right),$$

$$n_{2lm}(k) = \delta_{m,0} \frac{2^l}{(2l-1)!!} \left(l + \frac{3}{2} \right) \times \left(\frac{(k/k_0)^2}{l + \frac{3}{2}} - 1 \right)^2 \left(\frac{k}{k_0} \right)^{2l} \exp\left(-\frac{k^2}{k_0^2}\right), \quad (12)$$

with $k_0^2 = M\omega_{\text{osc}}$. In this approach we still have plane-wave initial states and simply use the shell model to determine their population. For a consistent calculation, the momentum distribution should not contain relativistic components; it must be cut off at some maximum (target nucleon) momentum, say, $k_{\max} \lesssim \frac{1}{2}M$. For the Fermi distribution, we can perform the above integrals exactly; the results are given in Appendix A.

For high $|\mathbf{q}|$ (say, $|\mathbf{q}| \gtrsim 2k_F$), we must employ relativistic kinematics to describe the recoil nucleon. Now for large energy loss, we should not use the effective mass for the recoiling nucleon, since it is well above the Fermi sea. For the final nucleon energy, we will therefore assume

$$\epsilon_{\mathbf{k}} = (k^2 + M^2)^{1/2}.$$

For the initial bound nucleon, we have

$$\epsilon_{\mathbf{k}} = k^2/2M + U(k^2) = k^2/2M^* + U(0),$$

where $U(k^2)$ is the effective single-particle potential in nuclear matter. In this form it is clear that the potential effectively shifts the electron energy loss ω to take into account the nuclear binding. Our approach will be to treat $U(k^2)$ as a constant $\bar{\epsilon}$. The final result should then be displaced toward the more inelastic region by this average separation energy $\bar{\epsilon}$, which will increase with \mathbf{q} and approach some constant value for very large \mathbf{q} (when the Pauli principle no longer restricts the recoiling nucleons). Finally, then, the energy-conserving δ function becomes

$$\delta[\omega + (M^2 + \mathbf{k}^2)^{1/2} - (M^2 + (\mathbf{k} + \mathbf{q})^2)^{1/2}] = \frac{\epsilon_{\mathbf{k}+\mathbf{q}}}{|\mathbf{k}| |\mathbf{q}|} \times \delta \left[u - \frac{M\omega}{|\mathbf{k}| |\mathbf{q}|} \left(1 + \frac{\omega}{2M} \right) + \frac{|\mathbf{q}|}{2|\mathbf{k}|} \left(1 - \frac{\omega}{M} \frac{|\mathbf{k}|^2}{|\mathbf{q}|^2} \right) \right],$$

where we still treat the *target* nucleon nonrelativistically, and where $u = \cos\tau$. We then have¹³

$$\begin{aligned}
 W_1(\mathbf{q}^2, \omega) &= \frac{3M_T}{4\pi A} \left(\frac{2\Omega}{3\pi^2 A} \right) \frac{2\pi}{|\mathbf{q}|} \int_0^\infty dk \frac{kn(k)}{(M^2+k^2)^{1/2}} \\
 &\quad \times \left\{ 1 - n \left[k^2 + 2M\omega \left(1 + \frac{\omega}{2M} \right) \right]^{1/2} \right\} \\
 &\quad \times \left(T_1(q^2) + \frac{1}{2} \frac{T_2(q^2)}{M^2} \left\{ k^2 - \left[\frac{M\omega}{|\mathbf{q}|} \left(1 + \frac{\omega}{2M} \right) - \frac{|\mathbf{q}|}{2} \right]^2 \right\} \right), \\
 W_2(\mathbf{q}^2, \omega) &= \frac{3M_T}{4\pi A} \left(\frac{2\Omega}{3\pi^2 A} \right) \frac{T_2(q^2)}{M^2} \frac{2\pi}{|\mathbf{q}|} \int_0^\infty dk \frac{kn(k)}{(M^2+k^2)^{1/2}} \\
 &\quad \times \left\{ 1 - n \left[k^2 + 2M\omega \left(1 + \frac{\omega}{2M} \right) \right]^{1/2} \right\} \\
 &\quad \times \left(\left\{ (M^2+k^2)^{1/2} - \frac{\omega}{|\mathbf{q}|} \left[\frac{M\omega}{|\mathbf{q}|} \left(1 + \frac{\omega}{2M} \right) - \frac{|\mathbf{q}|}{2} \right]^2 \right\} \right. \\
 &\quad \left. + \frac{1}{2} \frac{q^2}{|\mathbf{q}|^2} \left\{ k^2 - \left[\frac{M\omega}{|\mathbf{q}|} \left(1 + \frac{\omega}{2M} \right) - \frac{|\mathbf{q}|}{2} \right]^2 \right\} \right). \quad (13)
 \end{aligned}$$

Again, these integrals can be performed for the Fermi distribution $n(k) = \theta(k_F - k)$; the quasielastic results are compiled in Appendix A.

B. Meson Production

Near pion threshold, Czyz and Walecka⁵ use the single-nucleon electroproduction amplitude of Fubini, Nambu, and Wataghin and the Fermi-gas excitation spectrum. Their amplitude is good only to order $1/M$ and consequently good only for low-energy pions. They compute both the coherent and incoherent cross sections for electron energy losses above meson threshold, but well below the 3-3 resonance. (The interactions of the pions with the nucleons is restricted to a single production event, also a good approximation for very low-energy pions.) If we neglect nuclear recoil corrections, the thresholds for these processes are $\omega = \mu$ for coherent π^0 production and

$$\omega = \mu + (|\mathbf{q}|/2M^*) (|\mathbf{q}| - 2k_F) \theta(|\mathbf{q}| - 2k_F) = \mu + \omega_{\min}$$

for incoherent production, where μ is the pion mass, and ω_{\min} again enters because of the finite momentum distribution. The reader is referred to Ref. 5 for the explicit forms of the cross sections near pion threshold; these will be commented upon in Sec. III.

We now look at pion electroproduction in the region of the 3-3 resonance and assume that N^* production dominates single-pion electroproduction. Further, we treat the $\frac{3}{2}^+$ nucleon isobar as a discrete state, described by a Rarita-Schwinger¹⁴ wave function $\omega_{\alpha\nu}(k)$ which

¹³ We have let $1 - \omega |\mathbf{k}|^2/M |\mathbf{q}|^2 = 1$ in the integrand. This is the only approximation used; for the Fermi distribution, $\omega |\mathbf{k}|^2/M |\mathbf{q}|^2 < 1$ throughout the range of integration for all $|\mathbf{q}| \geq 2k_F$.

¹⁴ W. Rarita and J. Schwinger, Phys. Rev. **60**, 61 (1941).

transforms like a four-component spinor on the α index and like a four-vector on the ν index (the spinor index is now suppressed); each vector component satisfies the Dirac equation. For the nuclear transition current, we now have¹⁵

$$J_\mu = \sum_{\mathbf{k}\lambda} b_{\mathbf{k}\lambda}^\dagger \langle \mathbf{k} + \mathbf{q} | \lambda' (N^*) | j_\mu | \mathbf{k} \lambda (N) \rangle a_{\mathbf{k}\lambda} \theta(k_F - |\mathbf{k}|), \quad (14)$$

where $b_{\mathbf{k}\lambda}^\dagger$ is a free isobar creation operator. For the nucleon-isobar transition current, we take the completely covariant gauge-invariant couplings of Gourdin and Salin¹⁶

$$\begin{aligned}
 (\Omega^2 EE')^{1/2} \langle k' = k + q, N^* | j_\mu(0) | k, N \rangle &= (MM')^{1/2} \\
 &\quad \times \bar{\omega}_\nu(k') \gamma_5 \{ i [C_3(q^2)/\mu] (q_\nu \gamma_\mu - q \delta_{\nu\mu}) \\
 &\quad - [C_4(q^2)/\mu^2] (k'_\mu q_\nu - k' \cdot q \delta_{\mu\nu}) - [C_5(q^2)/\mu^2] \\
 &\quad \times (k_\mu q_\nu - k \cdot q \delta_{\mu\nu}) \} u(k), \quad (15)
 \end{aligned}$$

where M' is the isobar mass. From photoproduction data,¹⁷ $C_3(0) = 0.298$; $C_4(0) + C_5(0) = -0.0336$, and only the C_3 coupling need be retained for small q^2 . If we now introduce the spin- $\frac{3}{2}$ projection operator and evaluate the trace, we again obtain Eq. (8), but with

$$\begin{aligned}
 T_1(q^2) &= \left[\left(\frac{C_3^n}{\mu} \right)^2 + \left(\frac{C_3^p}{\mu} \right)^2 \right] \frac{(M' - M)^2 + q^2}{4} \\
 &\quad \times \left[(M' + M)^2 + \frac{1}{3} \left(\frac{M(M + M') + q^2}{M'} \right)^2 \right], \\
 T_2(q^2) &= \left[\left(\frac{C_3^n}{\mu} \right)^2 + \left(\frac{C_3^p}{\mu} \right)^2 \right] \frac{2}{3} M^2 q^2 \\
 &\quad \times \left(2 + \frac{1}{2M'^2} (q^2 - M'^2 + M^2) \right). \quad (16)
 \end{aligned}$$

The form factor $C_3^n(q^2) = C_3^p(q^2) = C_3(q^2)$ is plotted¹⁸ in Fig. 2 and will be discussed in Sec. III.

An easier way of going from the relativistic form of the vertex Eq. (15) to the $T_{1,2}(q^2)$ is to use the Bjorken-Walecka (BW)¹⁹ prescription. They give the general form of the vertex function in terms of three scalar form factors $g_{1,2,3}(q^2)$ [see BW, Eq. (2.18)] and relate these to the helicity amplitudes f_\pm, f_c [BW, Eq. (6.9)]. In terms of the latter,

$$\begin{aligned}
 T_1(q^2) &= M'^2 [|f_+|^2 + |f_-|^2], \\
 T_2(q^2) &= M^2 [(2q^4/q^{*4}) |f_c|^2 + (q^2/q^{*2}) (|f_+|^2 + |f_-|^2)], \quad (17)
 \end{aligned}$$

¹⁵ We no longer require the recoil momentum to be outside the Fermi sphere, although decay of the N^* might be inhibited by the Pauli principle.

¹⁶ M. Gourdin and Ph. Salin, Nuovo Cimento **27**, 193 (1963); **27**, 300 (1963).

¹⁷ J. Mathews, Phys. Rev. **137**, B444 (1965).

¹⁸ J. D. Walecka and P. A. Zucker, Phys. Rev. **167**, 1479 (1968).

¹⁹ J. D. Bjorken and J. D. Walecka, Ann. Phys. (N.Y.) **38**, 35 (1966).

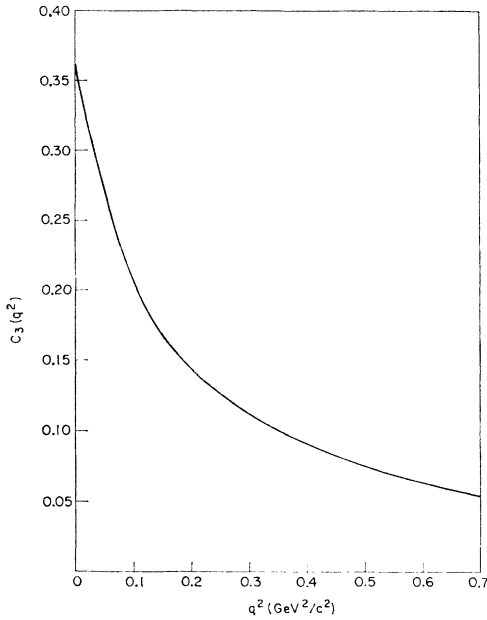


FIG. 2. Nucleon-isobar transition form factor from Ref. 18.

where the magnitude squared of the three-momentum transfer in the isobar rest frame is

$$q^{*2} = \{[(M'+M)^2+q^2]/2M'\} \{[(M'-M)^2+q^2]/2M'\}.$$

Therefore, we need only compare the form of the vertex given above with that given by Bjorken and Walecka, obtain the relation between the $f_{\pm,c}$ and the $C_{3,4,5}$, and write down $T_{1,2}(q^2)$ from Eq. (17):

$$f_c = \left(\frac{2}{3}\right)^{1/2} \frac{[(M'-M)^2+q^2][(M'+M)^2+q^2]^{1/2}}{4M'^2} \\ \times \left[\frac{C_3}{\mu} + \frac{C_4}{\mu^2} \left(\frac{M'^2-M^2-q^2}{2M'} \right) + \frac{C_4+C_5}{\mu^2} \left(\frac{M'^2+M^2+q^2}{2M'} \right) \right], \\ f_+ = - \frac{[(M'-M)^2+q^2]^{1/2}}{2M'} \\ \times \left((M'+M) \frac{C_3}{\mu} - q^2 \frac{C_4}{\mu^2} + \frac{C_4+C_5}{2\mu^2} (M'^2-M^2+q^2) \right), \quad (18) \\ f_- = \left(\frac{4}{3}\right)^{1/2} \frac{[(M'-M)^2+q^2]^{1/2}}{4M'} \left[\frac{C_3}{\mu} \left(\frac{M(M+M')+q^2}{M'} \right) \right. \\ \left. + q^2 \frac{C_4}{\mu^2} - \frac{C_4+C_5}{2\mu^2} (M'^2-M^2+q^2) \right].$$

It should be noted that, given a relativistic form of the vertex in terms of any set of form factors, this prescription allows us to calculate immediately the contribution of *any* isobar to the electron-nucleus cross section (since the remaining factors in $W_{1,2}$ involve just the isobar mass).

We must again perform the integrals given by Eq. (10), where $\epsilon_{\mathbf{k}+\mathbf{q}}$ is now the free-particle energy of an isobar with momentum $\mathbf{k}+\mathbf{q}$. But to produce the isobar from a nucleon at rest, the electron must provide a minimum three-momentum transfer of $(M'^2-M^2)/2M$ (≈ 350 MeV for the first πN resonance), and we shall use relativistic kinematics for the isobar. As in the high- $|\mathbf{q}|$ quasielastic case, we neglect the effective mass in the target states and expect to shift the results by $\bar{\epsilon}$ (again, this is really in the energy-conserving δ function). Carrying out the angular integrations, we have the same results as above in Eq. (13), except that we let $\omega(1+\omega/2M) \rightarrow \omega[1+\omega/2M - (1/2M)(M'^2-M^2)]$; we drop the $1-n(\mathbf{k}+\mathbf{q})$ term; and of course we replace the elastic form factors $T_{1,2}$ by the isobar expressions Eq. (17). The integrals are evaluated for the Fermi distribution and presented in Appendix A.

III. NUMERICAL RESULTS

In calculating the cross sections for various experimental conditions, the elastic and inelastic form factors must be specified. For the elastic form factors, we use the standard "dipole fit"²⁰

$$G_E^P = \frac{G_M^P}{2.79} = \frac{4M^2}{q^2} \frac{G_E^N}{1.91} = \frac{G_M^N}{-1.91} \\ = \left(1 + \frac{q^2}{0.71 \text{ GeV}^2} \right)^{-2},$$

where $G_E = F_1 - (q^2/2M)F_2$ and $G_M = F_1 + 2MF_2$. For the inelastic form factor $C_3(q^2)$, we use the relativistic N/D calculation of Walecka and Zucker.¹⁸ They keep π , N , and ω exchange graphs as the excitation mechanism, with one unknown parameter ($g_{\omega\pi\gamma}g_{\omega NN}$), and obtain a good fit to all the existing inelastic electron-proton scattering data. The form factor is plotted in Fig. 2.

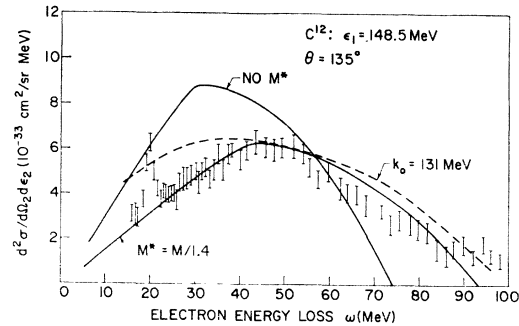


FIG. 3. Data are those of Leiss and Taylor, taken from Ref. 3, for C^{12} quasielastic peak with incident electron energy 148.5 MeV and electron scattering angle 135° . Solid curves are the Fermi-gas results with no effective mass and with the nuclear matter effective mass $M^* = M/1.4$. Dashed curve is for harmonic-oscillator momentum distribution (no effective mass is used here). All curves calculated with $k_F = \frac{1}{4}M$.

²⁰ This may not be a good representation for $G_E^N(q^2)$ for $q^2 > 1 \text{ GeV}^2$. See G. Weber, in *Proceedings of the 1967 International Symposium on Electron and Photon Interactions at High Energies* (Stanford Linear Accelerator Center, Stanford, Calif., 1968).

Figures 3-5 display the results for a wide range of experimental conditions. In Fig. 3, the data are those of Leiss and Taylor, published in Fig. 7 of Ref. 3. The solid curves are those for the Fermi distribution, in one case with $M^*=M/1.4$, in the other with no effective mass; the dashed curve is calculated using the harmonic-oscillator C^{12} distribution

$$n(k) = [1 + \frac{1}{3}(k/k_0)^2] \exp(-k^2/k_0^2),$$

with $k_0=131$ MeV. In this case, the contribution from each shell should be displaced by its binding energy. Since these data are in the small-energy-loss regime, the arguments of Sec. II suggest that we use the nuclear-matter value²¹ $M^*=M/1.4$. Alternatively, we could interpret M^* as a variable parameter, adjusted to locate the peak at the experimental value, but we would again obtain $M^*=M/1.4$ for this case. It should be noted once more that the effective-mass calculation cannot give the detailed threshold behavior, as is evidenced in Fig. 3 by the appearance of the giant resonance. A convenient prescription is, for $|\mathbf{q}| \lesssim k_F$, to use the nuclear-matter effective mass, but for $|\mathbf{q}| \gtrsim 2k_F$ to neglect the effective mass and displace the curves by the separation energy $\bar{\epsilon}$. In the latter case, the quasielastic peak may be used to set $\bar{\epsilon}$. This is done in Fig. 4: The solid curves are the quasielastic and isobar production results calculated here and the threshold result of Ref. 5; the data are those of Zimmerman²²; and the dashed curve indicates a displacement of $\bar{\epsilon} \sim 35$ MeV to fit the quasielastic peak.

Above meson threshold, data become very scarce. An important result is that the Czyz-Walecka calculation indicates that pion production is very small (compared to typical quasielastic cross sections) for at least 25 or 30 MeV above threshold. This can be significant for extracting information on dynamical

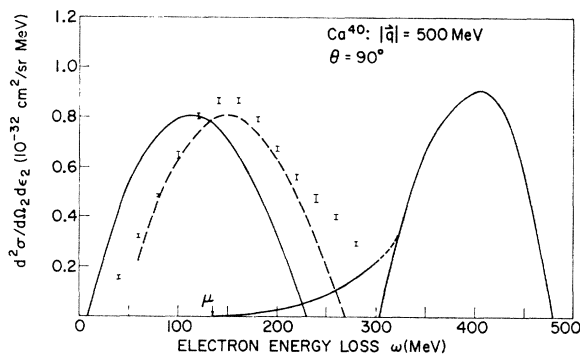


FIG. 4. Data are those of Zimmerman for Ca^{40} with constant three-momentum transfer $|\mathbf{q}|=500$ MeV and electron scattering angle 90° . Solid curves are the Fermi-gas results for the quasi-elastic, pion threshold, and isobar calculations. Dashed curve indicates displacement ~ 35 MeV to fit quasielastic peak.

²¹ M. Kawai and K. Kikuchi, *Nuclear Matter and Nuclear Reactions* (North-Holland Publishing Co., Amsterdam, 1968).

²² P. D. Zimmerman, thesis, Stanford University, 1969 (unpublished).

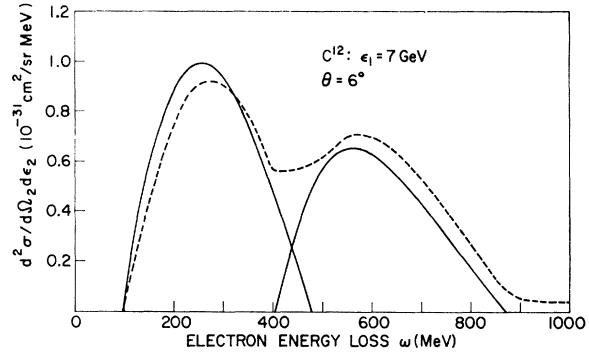


FIG. 5. Fermi-gas results for quasielastic and isobar contributions for incident electron energy 7 GeV and electron scattering angle 6° . Dashed curve is the "radiated" or raw cross section (calculated with $\Delta\epsilon=10$ MeV; see Appendix B).

correlations in the far quasielastic region. In Fig. 5, the solid curves are the Fermi-gas results for a very high incident energy; the dashed curve is the "radiated" cross section (see Appendix B). In any case, it is hoped that a careful experimental study will be carried out into the region of pion production. This, together with a more realistic theoretical analysis, can yield considerable new information. A very interesting calculation will be to estimate the effects of isobar-nucleon interactions on the cross section.

In summary, the inelastic electron-nucleus cross section has been calculated in three different regions of energy loss, using the same (Fermi-gas) nuclear model. In the quasielastic region, the electron scatters elastically from individual nucleons; for threshold pions, the Fubini-Nambu-Wataghin single-nucleon electroproduction amplitude is used, and pion-nucleon interactions are restricted to the production event; in the region of the first resonance, isobar excitation is considered to dominate. These results are model-dependent and should allow some insight into the nuclear physics. For example, the cross sections would appear considerably different if the chief mode of energy loss were excitation of collective oscillations.

ACKNOWLEDGMENTS

It is a pleasure to express thanks to Dr. T. W. Donnelly for interesting discussions on the quasielastic results, to Peter Zimmerman for supplying the experimental data of Fig. 4 prior to publication, and especially to Professor J. D. Walecka for suggesting this calculation and for his many helpful comments.

APPENDIX A

We here collect the results for the Fermi distribution

$$(\frac{d^2\sigma}{d\Omega_2 d\epsilon_2})_{\text{lab}} = (Z^2\sigma_M/M_T)$$

$$\times [W_2(\mathbf{q}^2, \omega) + 2W_1(\mathbf{q}^2, \omega) \tan^2 \frac{1}{2}\theta],$$

where M_T is the target (nuclear) mass, Z is the nuclear charge, \mathbf{q} is the three-momentum transfer to the

nucleus in the lab frame, $\omega = \epsilon_1 - \epsilon_2$ is the electron energy loss, and the Mott cross section is $\sigma_M = (\alpha^2 \cos^2 \frac{1}{2}\theta) / 4\epsilon_1^2 \sin^4 \frac{1}{2}\theta$, with ϵ_1 (ϵ_2) the initial (final) electron energy.

Quasielastic Contribution

$$T_1(q^2) = \frac{1}{2}q^2(F_1^p + 2MF_2^p)^2 + \frac{1}{2}q^2(F_1^n + 2MF_2^n)^2,$$

$$T_2(q^2) = 2M^2(F_1^p + q^2F_2^p)^2 + 2M^2(F_1^n + q^2F_2^n)^2,$$

where M is the nucleon mass, $q^2 = 4\epsilon_1\epsilon_2 \sin^2 \frac{1}{2}\theta$, and $F_{1,2}^{n,p}$ are the usual nucleon form factors. Let $Q \equiv |\mathbf{q}|/k_F$.

If $Q < 2$. Let $\nu \equiv M^* \omega / k_F^2$.

$$\begin{aligned} W_1(\mathbf{q}^2, \omega) &= \frac{3M_T}{4\pi A k_F^3} \frac{M^* k_F}{M(M+\omega)} \frac{\pi}{Q} \\ &\times \left\{ T_1(q^2) + \frac{1}{4} \frac{k_F^2}{M^2} T_2(q^2) \left[1 - \left(\frac{\nu}{Q} - \frac{Q}{2} \right)^2 \right] \right\} \\ &\times \left[1 - \left(\frac{\nu}{Q} - \frac{Q}{2} \right)^2 \right] \text{ if } \frac{1}{2}(2Q - Q^2) \leq \nu \leq \frac{1}{2}(2Q + Q^2) \\ &= \frac{3M_T}{4\pi A k_F^3} \frac{M^* k_F}{M(M+\omega)} \frac{\pi}{Q} 2\nu \\ &\times \left\{ T_1(q^2) + \frac{1}{2} \frac{k_F^2}{M^2} T_2(q^2) \left[1 - \nu - \left(\frac{\nu}{Q} - \frac{Q}{2} \right)^2 \right] \right\} \\ &\text{if } 0 \leq \nu \leq \frac{1}{2}(2Q - Q^2) \\ &= 0 \text{ if } \nu \geq \frac{1}{2}(Q^2 + 2Q), \end{aligned}$$

where M^* is the effective (nucleon) mass in the nuclear matter, A is the number of nucleons, and k_F is the Fermi momentum.

$$\begin{aligned} W_2(\mathbf{q}^2, \omega) &= \frac{3M_T}{4\pi A k_F^3} \frac{M^* k_F}{M(M+\omega)} \frac{\pi}{Q} \frac{k_F^2}{M^2} T_2(q^2) \\ &\times \left[1 - \left(\frac{\nu}{Q} - \frac{Q}{2} \right)^2 \right] \left\{ \left[\frac{M}{k_F} - \frac{\omega}{|\mathbf{q}|} \left(\frac{\nu}{Q} - \frac{Q}{2} \right) \right]^2 + \frac{1}{4} \frac{q^2}{|\mathbf{q}|^2} \right\} \\ &\times \left[1 - \left(\frac{\nu}{Q} - \frac{Q}{2} \right)^2 \right] \text{ if } \frac{1}{2}(2Q - Q^2) \leq \nu \leq \frac{1}{2}(2Q + Q^2), \\ &= \frac{3M_T}{4\pi A k_F^3} \frac{M^* k_F}{M(M+\omega)} \frac{\pi}{Q} \frac{k_F^2}{M^2} T_2(q^2) 2\nu \\ &\times \left\{ \left[\frac{M}{k_F} - \frac{\omega}{|\mathbf{q}|} \left(\frac{\nu}{Q} - \frac{Q}{2} \right) \right]^2 + \frac{1}{2} \frac{q^2}{|\mathbf{q}|^2} \right\} \\ &\times \left[1 - \nu - \left(\frac{\nu}{Q} - \frac{Q}{2} \right)^2 \right] \text{ if } 0 \leq \nu \leq \frac{1}{2}(2Q - Q^2) \\ &= 0 \text{ if } \nu \geq \frac{1}{2}(Q^2 + 2Q). \end{aligned}$$

If $Q \geq 2$. Let $\nu \equiv (M\omega/k_F^2)(1 + \omega/2M)$.

$$\begin{aligned} W_1(\mathbf{q}^2, \omega) &= \frac{3M_T}{4\pi A k_F^3} \frac{2\pi}{Q} \\ &\times \left\{ \left[T_1(q^2) - \frac{1}{2} \frac{k_F^2}{M^2} T_2(q^2) \left(\frac{\nu}{Q} - \frac{Q}{2} \right)^2 \right] \right. \\ &\times \left[\left(\frac{M^2}{k_F^2} + 1 \right)^{1/2} - \left(\frac{M^2}{k_F^2} + \left(\frac{\nu}{Q} - \frac{Q}{2} \right)^2 \right)^{1/2} \right] + \frac{1}{6} \frac{k_F^2}{M^2} T_2(q^2) \\ &\times \left[\left(2 \frac{M^2}{k_F^2} - \left(\frac{Q}{2} - \frac{\nu}{Q} \right)^2 \right) \left(\frac{M^2}{k_F^2} + \left(\frac{\nu}{Q} - \frac{Q}{2} \right)^2 \right)^{1/2} \right. \\ &\left. \left. - \left(2 \frac{M^2}{k_F^2} - 1 \right) \left(\frac{M^2}{k_F^2} + 1 \right)^{1/2} \right] \right\} \text{ if } 0 \leq \nu \leq \frac{1}{2}(2Q - Q^2) \\ &= 0 \text{ otherwise.} \end{aligned}$$

$$\begin{aligned} W_2(\mathbf{q}^2, \omega) &= \frac{3M_T}{4\pi A k_F^3} \frac{k_F^2}{M^2} T_2(q^2) \frac{2\pi}{Q} \\ &\times \left(\frac{1}{3} \left\{ \left(\frac{M^2}{k_F^2} + 1 \right)^{3/2} - \left[\frac{M^2}{k_F^2} + \left(\frac{\nu}{Q} - \frac{Q}{2} \right)^2 \right]^{3/2} \right\} \right. \\ &+ \frac{\omega^2}{|\mathbf{q}|^2} \left(\frac{\nu}{Q} - \frac{Q}{2} \right)^2 \left\{ \left(\frac{M^2}{k_F^2} + 1 \right)^{1/2} \left[\frac{M^2}{k_F^2} + \left(\frac{\nu}{Q} - \frac{Q}{2} \right)^2 \right]^{1/2} \right\} \\ &\left. - \frac{\omega}{|\mathbf{q}|} \left(\frac{\nu}{Q} - \frac{Q}{2} \right) \left[1 - \left(\frac{\nu}{Q} - \frac{Q}{2} \right)^2 \right] \right) \\ &+ \frac{1}{6} \frac{q^2}{|\mathbf{q}|^2} \left\{ \left[2 \frac{M^2}{k_F^2} - \left(\frac{\nu}{Q} - \frac{Q}{2} \right)^2 \right] \left[\frac{M^2}{k_F^2} + \left(\frac{\nu}{Q} - \frac{Q}{2} \right)^2 \right]^{1/2} \right. \\ &\left. - \left(2 \frac{M^2}{k_F^2} - 1 \right) \left(\frac{M^2}{k_F^2} + 1 \right)^{1/2} \right\} - \frac{1}{2} \frac{q^2}{|\mathbf{q}|^2} \left(\frac{\nu}{Q} - \frac{Q}{2} \right)^2 \\ &\times \left\{ \left(\frac{M^2}{k_F^2} + 1 \right)^{1/2} - \left[\frac{M^2}{k_F^2} + \left(\frac{\nu}{Q} - \frac{Q}{2} \right)^2 \right]^{1/2} \right\} \\ &\text{if } \frac{1}{2}(Q^2 - 2Q) \leq \nu \leq \frac{1}{2}(Q^2 + 2Q) \\ &= 0 \text{ otherwise.} \end{aligned}$$

Isobar Contribution ($Q \geq 2$)

$$T_1(q^2) = M'^2 (|f_+|^2 + |f_-|^2),$$

$$T_2(q^2) = M^2 \left(2 \frac{q^4}{q^{*4}} |f_c|^2 + \frac{q^2}{q^{*2}} (|f_+|^2 + |f_-|^2) \right),$$

where M' is the isobar mass and

$$q^{*2} = \left(\frac{(M' + M)^2 + q^2}{2M'} \right) \left(\frac{(M' - M)^2 + q^2}{2M'} \right).$$

For the N^* (1236), keeping only the C_3 coupling of

Gourdin and Salin (this should be good for $q^2 \lesssim 1 \text{ GeV}^2$),

$$T_1(q^2) = 2 \left(\frac{C_3(q^2)}{\mu} \right)^2 \frac{(M' - M)^2 + q^2}{4} \\ \times \left[(M' + M)^2 + \frac{1}{3} \left(\frac{M(M + M') + q^2}{M'} \right)^2 \right]$$

$$T_2(q^2) = 2 \left(\frac{C_3(q^2)}{\mu} \right)^2 \frac{2}{3} M^2 q^2 \left(2 + \frac{1}{2M'^2} (q^2 - M'^2 + M^2) \right).$$

(The results immediately above are the only ones which pertain specifically to the $\frac{3}{2}^+$ isobar; the expressions for $T_{1,2}$ in terms of the Bjorken-Walecka helicity amplitudes and the expressions below for $W_{1,2}$ apply to any isobar.) $W_1(\mathbf{q}^2, \omega)$ and $W_2(\mathbf{q}^2, \omega)$ have the same form here as the $Q \geq 2$ quasielastic results above, except that we redefine

$$\nu = \left[\frac{M\omega}{k_F^2} \left(1 + \frac{\omega}{2M} \right) - \frac{M'^2 - M^2}{2k_F^2} \right].$$

APPENDIX B

Experimental studies of this type are severely hampered by the difficulty in applying radiative corrections to high-energy inelastic scattering results. The problem is that one must then include the correction from high-energy bremsstrahlung with correspondingly low-energy loss, and this will be a large correction when the cross section is very large at the lower excitation energy. However, this correction involves integrations (on ω_k) over the nuclear cross sections

$$(d^2\sigma/d\epsilon_2 d\Omega_2)(\epsilon_1 - \omega_k, \epsilon_2, \theta)$$

and

$$(d^2\sigma/d\epsilon_2 d\Omega_2)(\epsilon_1, \epsilon_2 + \omega_k, \theta),$$

where ω_k is the energy of the radiated photon, and

$$(d^2\sigma/d\epsilon_2 d\Omega_2)(\epsilon_1, \epsilon_2, \theta)$$

is just what the experimenter is trying to measure. An approach which suggests itself is to use the model given here for the nuclear cross section and "radiate" it, giving a prediction for the "raw" experimental data. If this reproduces the main features of the data, the model can then be used to calculate explicitly the high-energy bremsstrahlung corrections for the particular experimental conditions.

This program is easily carried through in a Meister-Griffy²³ approach. Here the radiated photons are classified as "soft" or "hard" according to whether they have an energy smaller or greater than some cutoff $\Delta\epsilon$. This cutoff must be small enough so that the variation in the cross section is small when the relevant energies are

²³ N. T. Meister and T. A. Griffy, Phys. Rev. **133**, B1032 (1954).

changed by $\Delta\epsilon$; thus the soft correction is directly proportional to the unradiated cross section, which we denote by

$$(d^2\sigma_0/d\Omega_2 d\epsilon_2)(\epsilon_1, \epsilon_2, \theta).$$

For the hard correction, denoted by

$$(d^2\sigma_h/d\Omega_2 d\epsilon_2)(\epsilon_1, \epsilon_2, \theta),$$

the variation in the cross section must be considered, but the peaking approximation can be used for the radiated photons. The cutoff $\Delta\epsilon$ should be chosen large enough so that the hard cross section is smaller than both the unradiated and radiated cross sections. Ideally, $\Delta\epsilon$ should then be varied to ensure that the sum of the hard and soft corrections (i.e., the radiated cross section) is unaffected over a reasonable range of $\Delta\epsilon$ values. The required expressions for this method are given very nicely by Henry²⁴ and will be repeated here for completeness. If we denote the radiated and the soft cross sections by subscripts R and s , respectively,

$$(d^2\sigma_R/d\epsilon_2 d\Omega_2)(\epsilon_1, \epsilon_2, \theta) = (d^2\sigma_h/d\epsilon_2 d\Omega_2)(\epsilon_1, \epsilon_2, \theta) \\ + (d^2\sigma_s/d\epsilon_2 d\Omega_2)(\epsilon_1, \epsilon_2, \theta) \\ = (d^2\sigma_h/d\epsilon_2 d\Omega_2)(\epsilon_1, \epsilon_2, \theta) + (1 + \delta_1) \\ \times e^{\delta_2} (d^2\sigma_0/d\epsilon_2 d\Omega_2)(\epsilon_1, \epsilon_2, \theta).$$

This can be "solved" for the unradiated cross section

$$\frac{d^2\sigma_0}{d\epsilon_2 d\Omega_2} = \left(\frac{d^2\sigma_R}{d\epsilon_2 d\Omega_2} - \frac{d^2\sigma_h}{d\epsilon_2 d\Omega_2} \right) (1 + \delta_1)^{-1} e^{-\delta_2},$$

where it must be remembered that the hard cross section involves integrations over the unradiated cross section. For the soft part, we have

$$\delta_1 = (\alpha/\pi) \left[(13/6) \ln(q^2/m^2) - \frac{1}{2} \ln(\epsilon_1/\epsilon_2) \right], \\ \delta_2 = (\alpha/\pi) \left[\ln(\Delta\epsilon^2/\epsilon_1\epsilon_2) \right] \left[\ln(q^2/m^2) - 1 \right],$$

where m is the electron mass. The hard part is given by

$$\frac{d^2\sigma_h}{d\epsilon_2 d\Omega_2}(\epsilon_1, \epsilon_2, \theta) = \frac{\alpha}{\pi} \int_{\Delta\epsilon}^{\omega_{k1}} d\omega_k \frac{1}{\epsilon_1} \left[\left(\frac{\epsilon_1 - \omega_k}{\omega_k} \right) \left(2 \ln \frac{2\epsilon_1}{m} - 1 \right) \right. \\ \left. + \frac{\omega_k}{\epsilon_1} \ln \frac{2\epsilon_1}{m} \right] \frac{d^2\sigma_0}{d\epsilon_2 d\Omega_2}(\epsilon_1 - \omega_k, \epsilon_2, \theta) + \frac{\alpha}{\pi} \int_{\Delta\epsilon}^{\omega_{k2}} \frac{d\omega_k}{\epsilon_2 + \omega_k} \\ \times \left[\frac{\epsilon_2}{\omega_k} \left(2 \ln \frac{2\epsilon_2}{m} - 1 \right) + \frac{\omega_k}{\epsilon_2 + \omega_k} \ln \frac{2\epsilon_2}{m} \right] \frac{d^2\sigma_0}{d\epsilon_2 d\Omega_2}(\epsilon_1, \epsilon_2 + \omega_k, \theta),$$

where

$$\omega_{k1} = \epsilon_1 - \epsilon_2 / [1 - (2\epsilon_2/M_T) \sin^2 \frac{1}{2}\theta]$$

and

$$\omega_{k2} = \epsilon_1 / [1 + (2\epsilon_1/M_T) \sin^2 \frac{1}{2}\theta] - \epsilon_2.$$

²⁴ G. R. Henry, Phys. Rev. **149**, 1217 (1966).